

DOI: 10.1002/cctc.201300467

Efficient Ruthenium Nanocatalysts in Liquid–Liquid Biphasic Hydrogenation Catalysis: Towards a Supramolecular Control through a Sulfonated Diphosphine–Cyclodextrin Smart Combination

Miguel Guerrero,^[a, b] Yannick Coppel,^[a, b] Nguyet Tran Thanh Chau,^[c, d] Alain Roucoux,^[c, d] Audrey Denicourt-Nowicki,^[c, d] Eric Monflier,^[e] Hervé Bricout,^[e] Pierre Lecante,^[f] and Karine Philippot^{*[a, b]}

The combination between a sulfonated diphosphine (L) and a cyclodextrin (CD) allowed the preparation of very stable water-soluble ruthenium nanoparticles (RuNPs) that displayed pertinent catalytic performances in hydrogenation of unsaturated substrates with a supramolecular control effect of the cyclodextrin. For comparison purpose, the RuNPs were produced by hydrogenation of the organometallic [Ru(1,5-cyclooctadiene)(1,3,5-cyclooctatriene)] complex under mild conditions (3 bar H₂; room temperature) and in the presence of L or a L/CD mixture as stabilizer leading to Ru/L and Ru/L/CD systems, respectively. The so-obtained nanoparticles were fully characterized by complementary techniques. Interestingly, NMR investigations evidenced 1) the strong coordination of the sulfo-

nated diphosphine ligand at the metallic surface and 2) in the presence of cyclodextrin, the formation of an inclusion complex between L and CD that modified the coordination mode of the diphosphine. The investigation of both RuNPs systems in biphasic hydrogenation of unsaturated substrates pointed out relevant differences in terms of reactivity, thus evidencing the influence of the supramolecular interaction at the metallic surface on the catalytic performances of the nanocatalysts. This work took advantage of the supramolecular properties of a cyclodextrin to modulate the surface reactivity of diphosphine-stabilized ruthenium nanoparticles and may open new opportunities in the field of nanocatalysis.

Introduction

The nanoparticles and nanotechnology field is a fast-growing research area that has already led to significant breakthroughs

with a wide variety of potential applications in biomedical, optical and electronic areas as well as in catalysis.^[1] During the past two decades, “nanocatalysis” has emerged as a modern area at the frontier between homogeneous and heterogeneous catalysis.^[2] This emergence results from the development of efficient synthesis methods based on the use of tools from molecular chemistry allowing to form better defined and also better characterized metal nanoparticles as catalysts.^[3]

Among numerous investigations of metal nanoparticles in catalysis, some of them are directly inspired from organometallic chemistry, with the use of metal–organic precursors as the source of metal atoms as well as of basic ligands (e.g., amines, phosphorous derivatives) to protect the metal surface and control the growth of the particles.^[4] Besides its role to obtain stable nanoparticles of controlled size, the ligand can also be chosen to transfer its physical-chemical properties to the nanoparticles systems, such as solubility or selectivity. In that context, our group and others have used original ligands able to tune the properties of metal nanoparticles of interest in organic catalysis.^[5] More recently, we have developed metal nanoparticles soluble in water (despite the sensitivity towards moisture of the organometallic complexes used as metal sources) by an adequate choice of water-soluble ligands such as 1,3,5-triaza-7-phosphaadamantane^[6] and alkyl sulfonated diphos-

[a] Dr. M. Guerrero, Dr. Y. Coppel, Dr. K. Philippot
CNRS
LCC (Laboratoire de Chimie de Coordination)
205, Route de Narbonne, F-31077 Toulouse (France)
Fax: (+33)561553003
E-mail: karine.philippot@lcc-toulouse.fr

[b] Dr. M. Guerrero, Dr. Y. Coppel, Dr. K. Philippot
Université de Toulouse
UPS, INPT, LCC
F-31077 Toulouse (France)

[c] Dr. N. T. T. Chau, Prof. A. Roucoux, Dr. A. Denicourt-Nowicki
Ecole Normale Supérieure de Chimie de Rennes
CNRS, UMR6226
Avenue du Général Leclerc, CS 50837, F-35708 Rennes cedex 7 (France)

[d] Dr. N. T. T. Chau, Prof. A. Roucoux, Dr. A. Denicourt-Nowicki
Université européenne de Bretagne

[e] Prof. E. Monflier, Dr. H. Bricout
UMR CNRS 8181
Université d'Artois, Faculté des Sciences Jean Perrin
Rue Jean Souvraz, SP 18 - F-62307 Lens Cedex (France)

[f] Dr. P. Lecante
CNRS
Centre d'Elaboration de Matériaux et d'Etudes Structurales (CEMES)
29, rue Jeanne Marvig, BP 4347, 31055 Toulouse Cedex (France)

 Supporting information for this article is available on the WWW under <http://dx.doi.org/10.1002/cctc.201300467>.

phines^[7] that were active in hydrogenation of unsaturated substrates, in aqueous/organic biphasic catalysis conditions.

In the present contribution, the main objective is to increase and modulate the catalytic performances of ruthenium nanocatalysts by addition of a suitable molecular receptor. For this purpose we used a cyclodextrin as coadditive in the synthesis of sulfonated diphosphine-stabilized metal nanoparticles. This idea derived from recent works in organometallic catalysis^[8] and nanocatalysis,^[9] in which cyclodextrins (CDs) have been successfully used as mass-transfer promoters to improve a catalytic reaction in aqueous/organic biphasic conditions. Spectroscopic studies have demonstrated that β -CD and randomly methylated (RAME)- β -CD can interact with sulfonated phosphines by forming inclusion complexes, thus tuning the catalytic performances of the metal centers.^[10] Our strategy then relied on the combination of the advantages of both a sulfonated diphosphine as efficient stabilizer for metal nanoparticles in aqueous solution and a cyclodextrin for its shuttle and supramolecular control effects in catalysis. The goal was to have highly stable metal nanoparticles in water to characterize the ligand L/CD association and to study its influence on the reactivity during hydrogenation reaction of aromatic model substrates, in terms of conversion and selectivity. Furthermore, this work integrates well in the principles of green chemistry by answering to a few aims as: high number of reactive sites at the surface of metal nanoparticles to increase catalytic performance, immobilization of the nanocatalysts in aqueous phase as an environmentally friendly way to produce organic compounds, use of an aqueous/organic biphasic process for recovering and recycling of the catalyst, and use of a smart combination between a ligand and a phase transfer promoter to improve selectivity through a supramolecular control.

Herein we thus report: 1) the synthesis of water-soluble ruthenium nanoparticles using either a sulfonated diphosphine or its combination with the RAME- β -CD, the latter of which, as far as we know, has been described here for the first time; 2) their characterization by liquid and solid-state NMR spectroscopy, elemental analysis, TEM, high-resolution (HR) TEM, wide-angle X-ray scattering (WAXS), and dynamic light scattering (DLS); and 3) the investigation of these nanosystems in hydrogenation reaction of poly-functional aromatic molecules (styrene, acetophenone, and *m*-methylanisole) in substrate-water biphasic conditions. This study evidences the influence of the cyclodextrin, if present, on the catalytic performances of the nanocatalysts compared to those obtained with diphosphine-stabilized nanocatalysts.

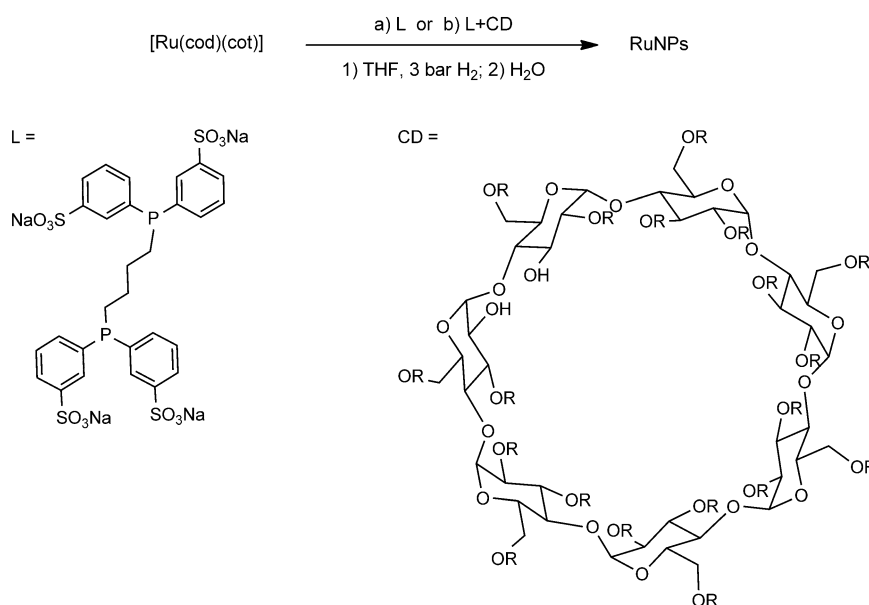
Results and Discussion

The ruthenium nanoparticles (RuNPs) were synthesized by the direct hydrogenation of the metal organic precursor [Ru(cod)-(cot)] (cod = 1,5-cyclooctadiene; cot = 1,3,5-cyclooctatriene) in THF under mild conditions (3 bar H₂; room temperature) in the presence of 1,4-bis[(di-*m*-sulfonatophenyl)phosphino]butane (L) as sulfonated diphosphine ligand (L) or a combination of this ligand with RAME- β -CD (Scheme 1).

These RuNPs have been characterized in solution by liquid NMR and dynamic light scattering (DLS), after isolation of the particles and dispersion in water. Grids were prepared from THF and aqueous solutions for TEM and high-resolution (HR) TEM analysis. The purified nanoparticles as powders were also characterized by solid-state NMR spectroscopy, elemental analysis, and wide-angle X-ray scattering (WAXS). The obtained results are hereafter presented as depending on the mode of stabilization used for the synthesis of the particles.

Synthesis and characterization of the sulfonated-diphosphine-stabilized RuNPs

First of all, the RuNPs were prepared by using the sulfonated diphosphine ligand L, in different [L]/[metal] molar ratio (0.1, 0.2, or 0.5, Scheme 1; method a). This sulfonated diphosphine, containing four carbon atoms between the two phosphorus atoms, was chosen according to the best catalytic results previously obtained with this ligand.^[7] The so-obtained RuNPs were found highly stable in THF solution, as no precipitation of bulk metal was observed at least after 3 months, thus demonstrating the efficiency of L in stabilizing the Ru⁰ nanoclusters. Afterwards, the nanoparticles were isolated as a black solid by precipitation from the THF colloidal solution through addition of pentane and, remarkably, they were easily redissolved in water. Aqueous colloidal solutions were used for characterization of



Scheme 1. Synthesis of the RuNPs systems. R = H or CH₃, degree of substitution = 1.8.

the particles in solution as well as for their investigation in catalytic hydrogenation reactions during which they were again found visually stable without observation of agglomerates. The excellent water solubility of these RuNPs and their high stability result from 1) the strong σ -coordination of the phosphorous atom to the metal surface (see below) and 2) coulombic repulsion of the charged sulfonated groups of the ligand molecules.

TEM analysis from colloidal solutions in THF and water revealed the presence of small and well-dispersed particles displaying a mean diameter between 1.2 and 1.5 nm, depending on the [L]/[metal] molar ratio (0.1, 0.2, and 0.5).^[7] These mean diameters correspond to the metallic cores of the particles as the ligand shells are not visible by TEM. Importantly, the transfer of the RuNPs into water did not induce any relevant change in dispersion and in their mean diameters as presented in Figure 1 for the [L]/[Ru] ratio of 0.1. The hexagonal close

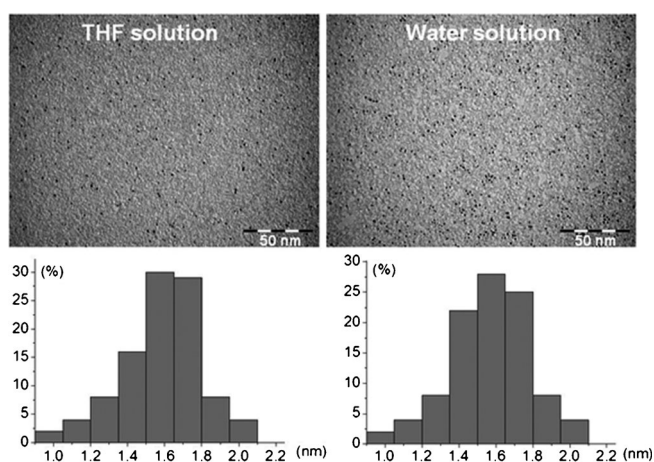


Figure 1. TEM analysis from colloidal solution in THF and water of RuNPs with [L]/[Ru] ratio = 0.1.

packed (hcp) structure of bulk Ru was determined by WAXS (Figure 2), with coherence lengths in the range 1.0–1.5 nm, in good agreement with the mean diameter measured by TEM. HRTEM analysis of RuNPs with [L]/[Ru] ratio of 0.1 from aqueous solutions revealed well-crystallized RuNPs with a mean di-

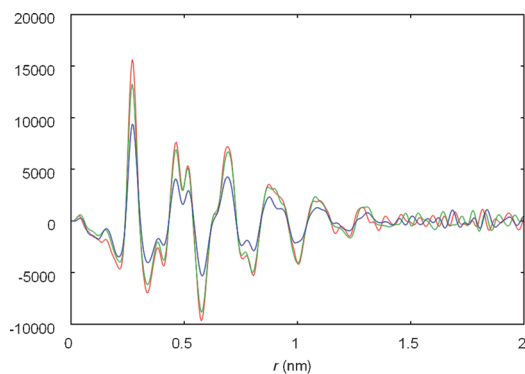


Figure 2. WAXS of RuNPs with [L]/[Ru] ratio = 0.1 (—), 0.2 (—), and 0.5 (—). r = rayon.

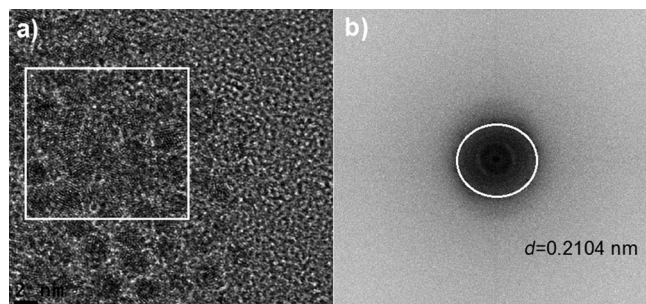


Figure 3. HRTEM analysis of RuNPs with [L]/[Ru] ratio = 0.1.

ameter of 1.5 nm as determined by TEM (Figure 3) and distances of inter-reticular planes in agreement with face-centered cubic (fcc) structure. However, they are single crystals displaying reticular planes extending over the entire particles. Well-oriented nanoparticles allowed us to measure the lattice parameters through fast-Fourier transform (FFT) spectroscopy indicating they were very close to the theoretical ones expected for the hcp structure of bulk Ru. Moreover, energy-dispersive X-ray analysis (EDX) performed during HRTEM studies revealed a characteristic pattern of metallic Ru (Supporting Information, Figure S1).

The RuNPs in aqueous solution were also analyzed by dynamic light scattering (DLS) giving interesting information on the nanoparticles dispersion in water (Figure 4). There is

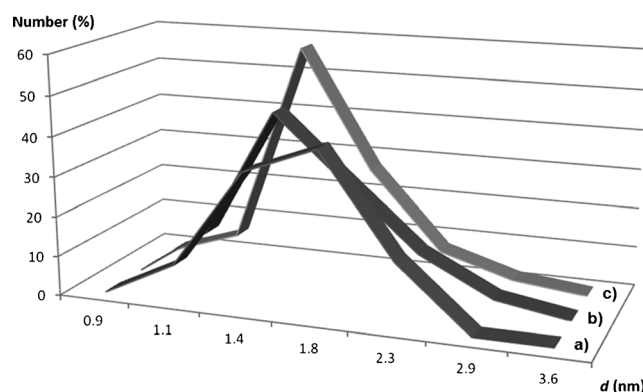


Figure 4. DLS analysis of RuNPs with [L]/[Ru] ratio = a) 0.1, b) 0.2, and c) 0.5.

a good correlation in the mean diameters of the nanoparticles obtained by DLS (1.5–1.8 nm) with those measured by TEM (1.2–1.5 nm). These results indicate that the NPs are isolated and do not agglomerate in water.

The interaction of L at the NPs surface was first characterized by ^1H and ^{31}P solution NMR performed on D_2O colloidal solutions containing RuNPs stabilized by L in the [L]/[Ru] = 0.1, 0.2, and 0.5 ratio. First of all, the ^1H NMR spectrum obtained for [L]/[Ru] = 0.1 (Figure S2) contained numerous sharp signals of very weak intensity, which can be attributed to the partial hydrogenation of the ligands owing to the reductive synthesis conditions (decomposition of the precursor under H_2), as previ-

ously observed with nonsulfonated L or other phosphines containing phenyl groups.^[11] On the ³¹P spectrum registered for [L]/[Ru]=0.1 (Figure S3), there was only a low sharp peak at $\delta=40.2$ ppm assigned to diphosphine oxide moieties free in solution but no signal was visible for the free diphosphine nor for the coordinated diphosphine. In solution NMR, the absence of signals for ligands coordinated to nanoparticles is generally attributed to several factors, including metal Knight shift owing to close proximity with the metal, fast T2 relaxation resulting from a diminution of the ligand tumbling at the nanoparticles surface, chemical exchange in the intermediate range of the chemical shift time scale and surface anisotropy.^[12]

Solution NMR studies performed on aqueous colloidal solutions containing higher amount of ligand (RuNPs prepared with [L]/[Ru] ratio of 0.2 and 0.5) gave also rise to the absence of signals for coordinated diphosphine as well as to the presence of signals for oxidized free diphosphine. However, in these cases, a sharp signal at $\delta=-15.2$ ppm was observed on the ³¹P NMR spectra with increased intensity if [L]/[Ru] increased (Figure S3). This signal has the expected chemical shift for the free ligand, which was confirmed by measuring the diffusion coefficient found equal to the one of L alone ($2.3 \pm 0.1 \times 10^{-10} \text{ m}^2 \text{ s}^{-1}$). These results suggest that there was no exchange between attached L ligands to the RuNPs surface and free L ligands in solution or if there was one, it was very slow at the NMR timescale. Recently, transfer NOE spectroscopy (trNOE) has been reported as a powerful NMR measurement for the characterization of grafted ligands at the nanoparticles surface in fast exchange with free ligands in solution.^[13] In the present case, only weak positive NOE or zero quantum artifacts were observed in the NOESY spectrum of a colloidal solution containing RuNPs prepared with 0.5 equivalents of L, typical of protons with high mobility. The absence of trNOE signals confirms that, if there was any exchange of L ligands coordinated to the surface of RuNPs with L molecules free in solution, this was relatively slow on the NMR timescales.

Finally, to obtain more information about the system, the nanoparticles were analyzed by cross-polarization magic angle spinning (CPMAS) solid-state NMR spectroscopy. The ³¹P CPMAS NMR spectrum of RuNPs with [L]/[Ru] ratio of 0.1 exhibited a broad signal between 30 and 60 ppm (Figure 5b) corresponding to the coordinated ligand through the two diphenylphosphino groups because no signal was detected at approximately -16 ppm, as observed for the free-ligand ³¹P NMR ($\delta=-15.8$ ppm; Figure 5a).

From all these results, we can conclude that the use of higher quantity than [L]/[Ru]=0.1 for the preparation of RuNPs stabilized by 1,4-bis[(di-*m*-sulfonatophenyl)phosphino]butane led to excess ligand that did not exchange with the coordinated molecules at the particle surface. Moreover, we previously observed in catalysis that a higher [L]/[Ru] ratio was not beneficial in terms of activity.^[7] For these reasons, in the continuation of this study, only the [L]/[Ru] ratio of 0.1 was considered.

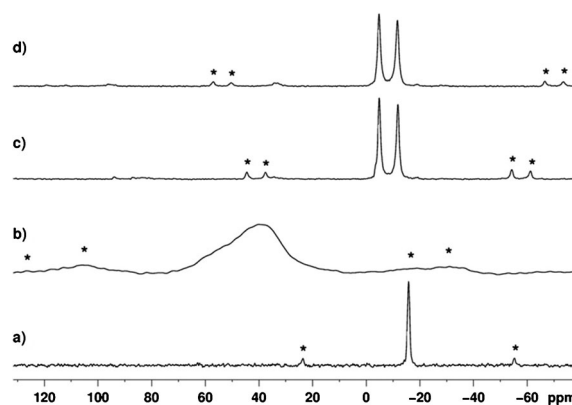


Figure 5. ³¹P CPMAS solid-state NMR of a) L, b) RuNPs stabilized by L with the [L]/[Ru] ratio = 0.1, c) mixture of L + CD, and d) RuNPs stabilized by L and CD with [Ru]/[L]/[CD] ratio = 1.0:0.1:1.0. ★: Spinning side bands.

Synthesis and characterization of the diphosphine L/RAME- β -CDs stabilized RuNPs

Inspired by previous observations with molecular catalysts in water, we attempted to modify the coordination properties of the sulfonated diphosphine L by adding an extra agent, namely a cyclodextrin (CD). Cyclodextrins are known for their shuttle effect and for modifying coordination properties of sulfonated diphosphines into molecular complexes thus tuning their catalytic performances.

A second set of experiments was then performed with a combination of 1,4-bis[(di-*m*-sulfonatophenyl)phosphino]butane (L) and RAME- β -CD (Scheme 1; method b). Several quantities of RAME- β -CD (0.2, 1.0, and 5.0 equiv.) were investigated. Considering the ability of CDs to form supramolecular inclusion entities with phosphine ligands of molecular complexes in aqueous media,^[10] a similar behavior could be expected with diphosphine-stabilized NPs. Our objective was then to study the influence of the CD in the reaction medium both on the stability of the sulfonated-diphosphine-stabilized RuNPs and on their catalytic properties that could result from a modification of the coordination of the diphosphine at the metal surface. For that purpose, the CD was added from the beginning of the RuNPs synthesis.

TEM and HRTEM analyses in water (Figure 6 and 7, respectively) of the [Ru]/[L]/[CD] nanoparticles did not reveal any difference in comparison with those of [Ru]/[L]. The nanoparticles were well-dispersed on the grids and displayed similar diameter and diameter distributions. They displayed distances between inter-reticular planes in accordance with the hcp structure.

The DLS measurements performed on the three L/CD-stabilized RuNPs samples ([Ru]/[L]/[CD] = 1.0:0.1:0.2, [Ru]/[L]/[CD] = 1.0:0.1:1.0, and [Ru]/[L]/[CD] = 1.0:0.1:5.0) gave rise to higher mean diameters than those of L-stabilized RuNPs obtained by previous measurements (Figure 8). However, the observed mean diameters were dependent upon the quantity of CD present during the particles synthesis, higher CD ratios leading to higher mean diameters. The hydrodynamic radii of the whole particles (that means the metallic cores with the ligand

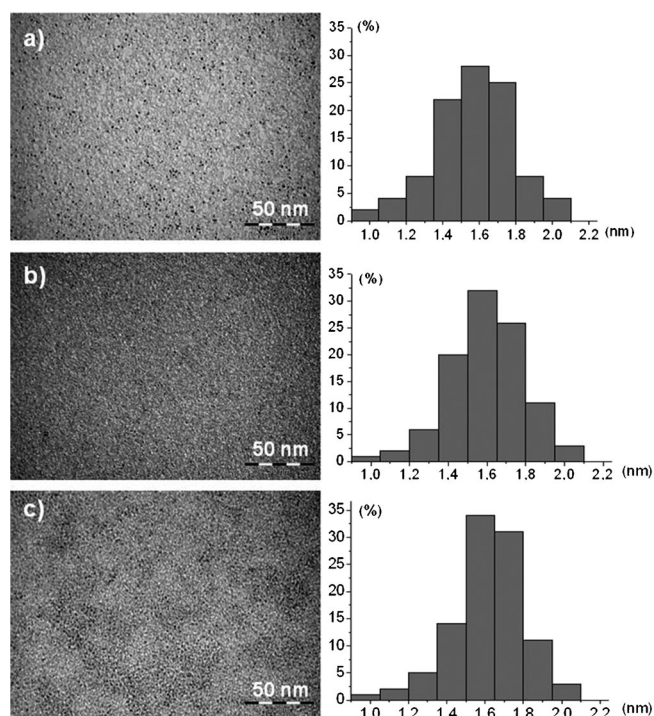


Figure 6. TEM analysis from colloidal solution water of RuNPs with [L]/[Ru] ratio = 0.1 and CD. a) [Ru]/[L]/[CDs] = 1.0:0.1:0.2, b) [Ru]/[L]/[CDs] ratio = 1.0:0.1:1.0, and c) [Ru]/[L]/[CDs] ratio = 1.0:0.1:5.0.

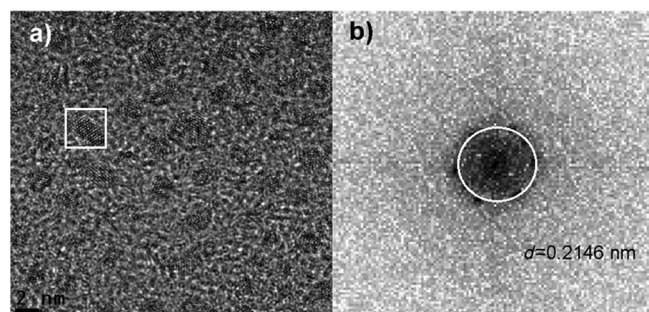


Figure 7. HRTEM analysis for the [Ru]/[L]/[CDs] (ratio = 1.0:0.1:0.2).

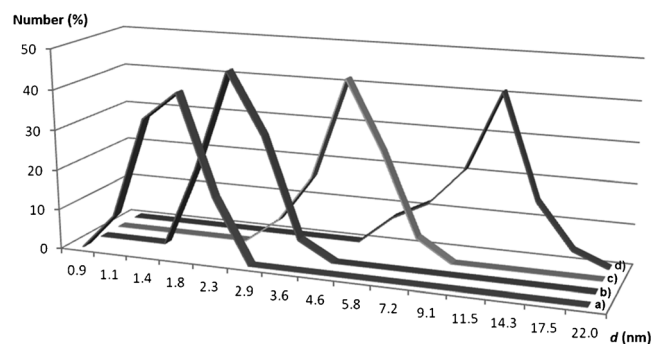


Figure 8. DLS analysis of RuNPs with [L]/[Ru] ratio = 0.1 and CD a) 0.0, b) 0.2, c) 1.0, and d) 5.0 equivalents.

shells) were determined by DLS, thus giving direct information on the influence of CD in the organization of the RuNPs in so-

lution. It appears clearly that CD surrounded the RuNPs. Considering the probable proximity of L and CD at the particle surface, a supramolecular interaction between L and CD could take place as previously observed for molecular complexes.^[10] To check the potential formation of an inclusion complex, between the aromatic rings of the diphosphine and the cavity of the RAME- β -CD cyclodextrin that could modulate the coordination properties of L, deep-NMR experiments were performed, in D₂O solution and in the solid state.

First of all, a mixture [L]/[CD] = 1.0 (without metal) was studied in the concentration conditions of the RuNPs synthesis. ¹H and ³¹P NMR spectra indicate a clear interaction between L and CD by resonance shifts if L and CD were mixed in D₂O (Figure S4 and S5). Only one set of ¹H NMR resonances were observed for CD and L suggesting the presence of a fast equilibrium between associated and dissociated states. The diffusion coefficient of CD was slightly reduced from $1.7 \pm 0.1 \times 10^{-10} \text{ m}^2 \text{ s}^{-1}$ to $1.5 \pm 0.1 \times 10^{-10} \text{ m}^2 \text{ s}^{-1}$, and that of L exhibited a more pronounced reduction from $2.3 \pm 0.1 \times 10^{-10} \text{ m}^2 \text{ s}^{-1}$ to $1.6 \pm 0.1 \times 10^{-10} \text{ m}^2 \text{ s}^{-1}$. Remarkably, intermolecular NOEs were observed between some CD protons and the aromatic protons of L (Figure S6). These NOEs could be related to the inclusion of one aromatic ring of L inside the cyclodextrin cavity as already described by some of us.^[10] We also observed that the initially positive intramolecular NOEs of L (Figure S6 left) became negative (Figure S6 right), thus indicating a decrease of the average local mobility of the L protons, owing to the interaction with CD. To summarize, all these data confirm the presence of a weak interaction between L and CD and a fast exchange (on the NMR timescale) between associated and dissociated states. Interestingly, this interaction could also be observed in the solid state, in which important modifications of ¹³C and ³¹P CPMAS NMR L resonances were detected in the presence of CD (Figure 5c). Notably the ³¹P CPMAS signal of L alone at $\delta = -15.8$ ppm was split in two resonances at $\delta = -11.7$ and $\delta = -4.8$ ppm for [L]/[CD] = 1.0. From these two phosphorus resonances that reveal the presence of two non-equivalent phosphorus atoms in the diphosphine ligands, we can assume the formation of an inclusion complex between the diphosphine and the CD, through an interaction of phenyl groups of L in the cavities of the CD molecules. However, the formation of this inclusion complex is not affected by excess CD.

Finally, NMR experiments were also performed with the RuNPs system prepared with L and CD in the ratio [Ru]/[L]/[CD] = 1.0:0.1:1.0, both in D₂O and in the solid state, giving rise to results very similar to the ones obtained for the mixture [L]/[CD] = 1.0 (Figure 5d and 9). Notably in the ³¹P CPMAS NMR spectrum, two major signals were observed at $\delta = -11.7$ and $\delta = -4.8$ ppm, as already detected for [L]/[CD] = 1.0. Furthermore, the broad signal between 30 and 60 ppm (Figure 5b) previously observed for the RuNPs prepared with a [Ru]/[L] = 0.1 ratio and attributed to coordinated diphosphines to the Ru surface was also detected but with a very weak intensity. Jointly, these results indicate that, in the presence of a large amount of free CD relative to diphosphine ([Ru]/[L]/[CD] = 1.0:0.1:5.0), L interacts more strongly with the CD molecules

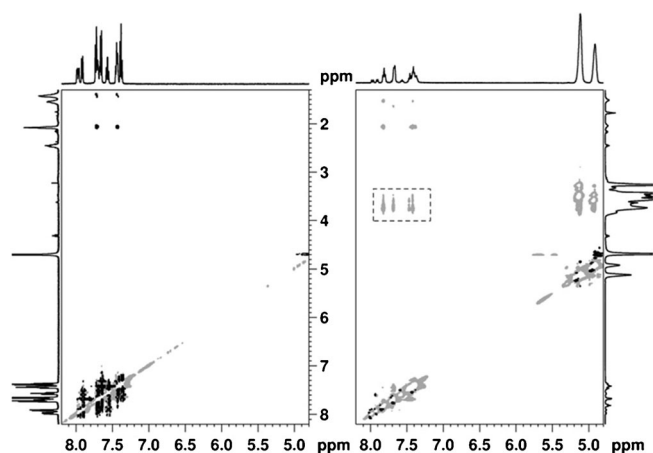


Figure 9. NOESY spectra of RuNPs stabilized by 0.5 equivalents of L (left) and by L and CDs with [L]/[CD] ratio = 5.0 (right). NOE cross-peaks between the aromatic L and CD protons are shown in the dotted rectangle.

than with the RuNPs. Thus, the use of a mixture of CD and L induced a strong diminution of the affinity of L for the RuNPs surface and, in consequence, CD molecules were probably close to the surface of RuNPs.

Additional NMR experiments performed after adding excess CD to a colloidal solution containing preformed sulfonated diphosphine stabilized RuNPs led to similar results for [Ru]/[L] nanoparticles (no change observed on the NMR spectra). These results point out that the coordination of the diphosphine at the nanoparticles' surface was very strong and was not modified by the postaddition of CDs. In summary, the inclusion complex L/CD can be formed only if the diphosphine and the CD are both present during the synthesis of the nanoparticles, thus influencing the coordination of the diphosphine at their surface and consequently their properties.

Application of the RuNPs in catalytic hydrogenation reactions

Owing to the synthesis conditions of our RuNPs (dihydrogen atmosphere), the presence of hydrides at their surface was expected. The titration of surface hydrides could be simply performed by investigating the particles as catalysts in the hydrogenation model reaction of norbornene with no extra hydrogen added. The measurement of the amount of alkane formed by GC analysis allowed determining the suitable quantity of hydrogen atoms for reducing the alkene, and further to calculate the H/surface Ru atomic ratio considering the nanoparticles mean diameter. The presence of hydrides at the surface of sulfonated-diphosphine-capped metal nanoparticles was previously confirmed with 1.6 hydrogen atoms per surface Ru atom for Ru/L.^[7] This value was herein determined for aqueous colloidal solutions of [Ru]/[L]/[CD] nanoparticles, giving rise to similar values (1.3, 1.3, and 1.2 for 0.2, 1.0, and 5.0 equiv. of CD, respectively). These results indicate that the nanoparti-

cles are able to activate dihydrogen and that whatever the quantity of CD used was, the number of hydrides per surface Ru atom is not affected.

To investigate the influence of the RAME- β -CD on the catalytic performances of our previously described sulfonated-diphosphine-stabilized nanomaterials, we chose to compare them in the catalytic hydrogenation of functionalized aromatic substrates, namely styrene, acetophenone, and *m*-methylanisole. The presence of CD should have an influence on the reactivity in terms of selectivity and kinetic properties. First, owing to the strong interaction between one phosphorous atom of the ligand and CD giving rise to an inclusion complex as demonstrated previously, the coordination of the ligand at the metal surface was modified in the presence of CD which can lead to different activity and selectivity. Secondly, the presence of CD in excess should help the transfer of the aromatic substrate towards the metallic surface through the hydrophobic cavity that can host organic compounds and further allow an increase the kinetic behavior of the hydrogenation reaction.

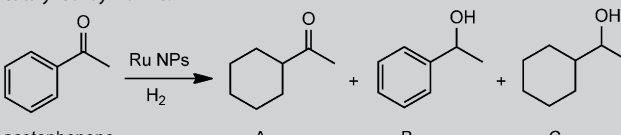
To study the influence on the reduction rate and chemoselectivity of diphosphine-stabilized nanoparticles chemically modified by CD, similar catalytic experiments were performed with both nanocatalysts Ru/L and Ru/L/CD. The hydrogenation reactions were performed in pure biphasic liquid-liquid conditions (substrate/water) with a [substrate]/[RuNPs] molar ratio of 100, at room temperature and under H₂ pressure (1 and 10 bar). The selectivities were determined by GC analysis. The results are summarized in Tables 1–3. It is noteworthy to mention that, given the number of surface Ru atoms was much lower than the total metal atoms present in the sample, the values given in Tables 1, 2, and 3 are underestimated. For example, if we consider the formation of full-shell clusters of ruthenium, the RuNPs of 1.6 nm have an approximate dispersion (D; the fraction of exposed Ru) value of approximately

Table 1. Styrene hydrogenation under hydrogen pressure catalyzed by RuNPs.^[a]

Entry	Nanocatalyst	H ₂ pressure [bar]	t [h]	Product selectivity ^[b] [%]			TON ^[c]	TOF ^[d] [h ⁻¹]
				ST	EB	EC		
1	Ru/L	1	40	0	0	100	71	2 (3)
2	Ru/L/0.2CD	1	40	0	0	100	178	5 (11)
3	Ru/L/1.0CD	1	40	0	0	100	591	15 (24)
4	Ru/L/5.0CD	1	40	0	9	91	2700	68 (108)
5	Ru/L	10	2	0	0	100	67	33 (57)
6	Ru/L/0.2CD	10	2	0	0	100	162	81 (142)
7	Ru/L/1.0CD	10	2	0	0	100	604	303 (473)
8	Ru/L/5.0CD	10	2	0	77	23	2448	1224 (2160)

[a] Reaction conditions: RuNPs (10 mg), styrene (3.9×10^{-3} mol), H₂ (1 or 10 bar), room temperature, water (10 mL). [b] EB = ethylbenzene; EC = ethylcyclohexane; ST = styrene, determined by GC analyses. [c] Initial TON is expressed as $\frac{\text{mol}_{\text{substrate converted}}}{\text{mol}_{\text{metal}}}$ (mol_{substrate converted} = 100%). [d] Initial TOF is expressed as $\frac{\text{mol}_{\text{substrate converted}}}{\text{mol}_{\text{metal}} \cdot \text{h}}$ and in brackets TOF is corrected for expression as $\frac{\text{mol}_{\text{substrate converted}}}{\text{mol}_{\text{surface Ru atoms}} \cdot \text{h}}$.

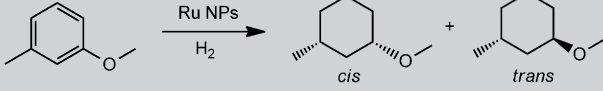
Table 2. Acetophenone hydrogenation under hydrogen pressure catalyzed by RuNPs.^[a]



Entry	Nanocatalyst	H ₂ pressure [bar]	t [h]	Products ^[b] [%]			TON ^[c]	TOF ^[d] [h ⁻¹]
				A	B	C		
1	Ru/L	1	20	0	84	16	71	4 (6)
2	Ru/L/0.2CD	1	20	3	86	11	151	8 (13)
3	Ru/L/1.0CD	1	20	6	82	12	414	21 (34)
4	Ru/L/5.0CD	1	20	9	91	0	567	28 (45)
5	Ru/L	10	2	0	0	100	71	36 (57)
6	Ru/L/0.2CD	10	2	0	0	100	178	89 (142)
7	Ru/L/1.0CD	10	2	14	52	34	514	257 (411)
8	Ru/L/5.0CD	10	2	14	60	26	1890	944 (1510)

[a] Reaction conditions: RuNPs (10 mg), acetophenone (3.9×10^{-3} mol), H₂ (1 or 10 bar), room temperature, water (10 mL). [b] Determined by GC analysis; A: 1-cyclohexylethanone, B: 1-phenylethanol, C: 1-cyclohexylethanol, determined by GC analysis. [c] Initial TON is expressed as $\text{mol}_{\text{substrate converted}} / \text{mol}_{\text{metal}}^{-1}$. [d] Initial TOF is expressed as $\text{mol}_{\text{substrate converted}} / \text{mol}_{\text{metal}}^{-1} \text{h}^{-1}$ and in brackets TOF is corrected for expression as $\text{mol}_{\text{substrate converted}} / \text{mol}_{\text{surface Ru atoms}}^{-1} \text{h}^{-1}$.

Table 3. Hydrogenation of 1-methoxy-3-methylbenzene (*m*-methylanisole).^[a]



Entry	Nanocatalyst	H ₂ pressure [bar]	t [h]	Conversion ^[b] [%]	Diastereomeric excess ^[b] [%]	TON ^[c]	TOF ^[d] [h ⁻¹]
2	Ru/L/0.2 CD	1	40	67	60	120	3 (5)
3	Ru/L/1.0CD	1	40	45	66	266	7 (11)
4	Ru/L/5.0CD	1	40	35	62	945	24 (38)
5	Ru/L	10	2	80	51	57	28 (45)
6	Ru/L/0.2CD	10	2	100	62	178	89 (142)
7	Ru/L/1.0CD	10	2	100	72	591	295 (472)
8	Ru/L/5.0CD	10	2	100	100	2700	1350 (2160)

[a] Reaction conditions: RuNPs (10 mg), methylanisole (3.9×10^{-3} mol), H₂ (1 or 10 bar), room temperature, water (10 mL). [b] Determined by GC analysis. [c] Initial TON is expressed as $\text{mol}_{\text{substrate converted}} / \text{mol}_{\text{metal}}^{-1}$. [d] Initial TOF is expressed as $\text{mol}_{\text{substrate converted}} / \text{mol}_{\text{metal}}^{-1} \text{h}^{-1}$ and in brackets TOF is corrected for expression as $\text{mol}_{\text{substrate converted}} / \text{mol}_{\text{surface Ru atoms}}^{-1} \text{h}^{-1}$.

0.62, indicating that approximately two-thirds of the total amount of Ru atoms are on the surface (which are active for the hydrogenation). Thus, we used this value to estimate turnover frequency (TOF) corrected by the fraction of surface metal atoms, given in brackets in Tables 1, 2, and 3.

The RuNPs systems (Ru/L; Ru/L/0.2CD; Ru/L/1.0CD; and Ru/L/5.0CD) were first evaluated in the hydrogenation of styrene (Table 1). Whatever the catalytic system, after 40 h under 1 bar H₂, both the *exo*-cyclic double bond and the aromatic ring were reduced giving rise to 100% conversion with a selectivity into ethylcyclohexane (EC) of 90–100%. Although all the other systems led to the complete formation of EC, the Ru/L/5.0CD

catalyst offered only 91% of totally reduced product, thus showing that a high amount of CD (5.0 equiv.) potentially tunes the kinetic behaviors and selectivities of the hydrogenation reaction. If the dihydrogen pressure was increased to 10 bar, comparable results were observed but the reaction was accelerated, with completion in only 2 h against 40 h under atmospheric pressure at room temperature. However, the Ru/L/5.0CD nanosystem presented a more pronounced difference with 77% of selectivity into ethylbenzene (EB) and 23% of EC compared with the results observed under 1 bar H₂. It appears that 5.0 equivalents of CD limit the total hydrogenation of styrene and that this effect is increased at higher pressure. This phenomenon could be explained by the formation of a competitive inclusion complex owing to the presence of a large excess of CD, which could wrap more efficiently the aromatic ring of styrene, thus limiting its hydrogenation in the same reaction time. According to the TOF values based on the amount of Ru introduced, CD-rich nanocatalysts finally appeared more active, thus evidencing the shuttle effect of the CD, which improves the approach of the C=C double bond of styrene towards the metal surface.

The second set of catalytic tests was performed with acetophenone, in similar reaction conditions (room temperature, 1 or 10 bar H₂). Under 1 bar H₂ (Table 2; entries 1–4), turnover number (TON) and TOF values tended to increase, showing a positive effect of the CD, compared to the values for the Ru/L nanocatalyst. In terms of selectivities, the 1-phenylethanol (B, 82–86%) was the major product but 1-cyclohexylethanol (A, 3%–9%) and 1-cyclohexylethanol (C, 11–16%) were also produced, which indicates that the hydrogenation of the aromatic cycle could take place.

However, no 1-cyclohexylethanol was detected with the Ru/L/5.0CD system. The increase in reaction pressure from 1 to 10 bar H₂ provided strong acceleration of the kinetic properties for all catalytic systems. As already observed under 1 bar H₂, TON and TOF values increased with higher quantity of CD. Concerning the selectivity, the total hydrogenated product (1-cyclohexylethanol; C) was obtained with 100% selectivity with Ru/L and Ru/L/0.2CD nanocatalysts after 2 h of reaction, whereas the systems more rich in CD (Ru/L/1.0CD and Ru/L/5.0CD) presented only 34 and 26% of C after the same time, indicating an influence of the CD on the course of the reaction at a suitable amount of CD (CD ≥ 1.0). 1-cyclohexylethanol (A) was also detected for Ru/L/CD with CD ≥ 1.0, in higher content than that observed under 1 bar H₂ (14% against 3–9%) for the catalytic systems Ru/L/0.2CD and Ru/L/1.0CD. Finally, according to the TOF values and as already seen for styrene, CD-rich nanocatalysts appear more active, thus evidencing the shuttle effect of the CD.

In summary, it appears that the presence of the cyclodextrin during the synthesis of the nanoparticles has an influence on the catalytic performances of the sulfonated-diphosphine-stabilized RuNPs in the hydrogenation of styrene and acetophe-

none, both in terms of activity and selectivity. First of all, the increasing TOF values with increasing CD content show that nanocatalysts more rich in CDs are more active, thus evidencing the shuttle effect of the CD. Nevertheless, we observed some differences depending on the quantity of CD. At a relatively low quantity of CD (0.2 equiv.), the effect was low. This can be explained by the fact that the CD was mainly involved in the formation of an inclusion complex with the diphosphine ligand at the metal surface, thus leading to stable RuNPs that were active but with no boosting effect. At higher quantity of CD, there was free CD in the reaction medium which improved the catalytic system, and this was even more pronounced with CD=5.0 compared to the situation with CD=1.0. Concerning the selectivity, we also noticed some differences if CD was present at a ratio $CD \geq 1.0$. In the case of styrene, a high quantity of CD (5.0 equiv.) limited the total hydrogenation of styrene, probably owing to the formation of an inclusion complex between the aromatic ring and the excess CD thus avoiding its hydrogenation in the same reaction time. In the case of acetophenone, the product selectivity tended also to vary with the CD content: $CD \geq 1$ contents led to higher quantities of partially hydrogenated products (1-phenylethanol and 1-cyclohexyl-ethanone) and this was even more pronounced with CD=5.0 equivalents. Interestingly, representative TEM images from colloidal solution in water of RuNPs after catalysis showed that the nanoparticles were not agglomerated (Figure S7).

The investigation in catalysis was pursued by studying the hydrogenation of a substrate of higher interest, namely 1-methoxy-3-methylbenzene (*m*-methylanisole). This disubstituted aromatic substrate was chosen to evaluate the influence of the CD on the reaction stereoselectivity because two diastereomeric products (*cis/trans*) can be formed. The catalytic reactions were performed at room temperature and under 1 or 10 bar H_2 (Table 3). The reaction presented slowly moderate conversions (18–67%) after 40 h, with the Ru/L nanocatalyst the less active. The highest conversion was observed for the nanocatalyst Ru/L/0.2CD with 67% of totally hydrogenated product after 40 h. As previously observed for styrene and acetophenone, higher quantities of CD led to lower conversions (45 and 35 for Ru/L/1.0CD and Ru/L/5.0CD, respectively) but higher TONs and TOFs were observed. Finally, as usually observed in the hydrogenation of aromatic derivatives with pure heterogeneous catalysts or aqueous colloidal suspensions, the formation of the thermodynamically less favorable *cis*-diastereomer was promoted with diastereomeric excesses up to 100%. Nevertheless, in all cases, we could observe a decrease in the diastereomeric excesses ($\approx 60\%$) after longer reaction times (40 h), indicating also the formation of the *trans* diastereoisomers through a probable roll-over mechanism.^[14] Whatever the system Ru/L/CD used, no significant difference was observed.

To increase the kinetic properties and the conversion rate in short times, the same experiments were also performed under 10 bar H_2 (Table 3). Undoubtedly, the hydrogenation of the aromatic cycle was accelerated, with better conversions (80–100%) after 2 h. The Ru/L nanocatalyst was also the less active (conversion 80%) but no difference in activity was observed

for the Ru/L/CD nanocatalysts whatever the quantity of CD was, all leading to 100% conversion in 2 h. TON and TOF values were also increased if higher quantities of CD were present in the reaction medium. Diastereomeric excesses between 50 and 100% were noticed, in favor of the kinetic *cis* product, evidencing that the quantity of CD had an influence on the selectivity of the reaction at higher hydrogen pressure, and the more CD-rich nanocatalysts (Ru/L/5.0CD) were the more selective.

All these results highlight the interest of combining a sulfonated diphosphine ligand with a cyclodextrin to tune the catalytic performances of RuNPs, as the formation of strong inclusion complexes between the ligand and/or the substrate within the cage of the cyclodextrin may lead to different selectivities and excess CD improve the activity through a mass-transfer promoter effect.

Conclusions

Sulfonated diphosphines were very efficient ligands for the stabilization of ruthenium nanoparticles (RuNPs) synthesized through the organometallic approach, giving rise to well-controlled nanoclusters in the diameter range 1.2–1.5 nm and displaying very low diameter dispersity. The water-solubility of the sulfonated diphosphine allowed obtaining very stable aqueous colloidal solutions (up to several months) by a simple transfer of the isolated particles into water. Deep-NMR studies conducted in the solid state as well as on the aqueous colloidal solutions evidenced the strong interaction of the sulfonated diphosphine ligand with the RuNPs surface. If a randomly methylated β -cyclodextrin was used as coadditive in the synthesis of the sulfonated-diphosphine-stabilized RuNPs, the formation of supramolecular inclusion complexes between the sulfonated diphosphine and cyclodextrin molecules was observed. The existence of an interaction between ligand and cyclodextrin was clearly evidenced by NMR spectroscopy (both in solution and in solid state), which appeared even stronger at higher cyclodextrin content, thus disrupting severely the coordination properties of the ligand towards the metal surface. However, it was observed that this interaction could take place only if the cyclodextrin is present during the synthesis of the particles.

The catalytic properties of the sulfonated diphosphine-stabilized RuNPs and sulfonated-diphosphine–cyclodextrin-stabilized RuNPs were compared in the hydrogenation reaction of unsaturated model substrates (styrene, acetophenone, and *m*-methylanisole) in biphasic liquid–liquid conditions. All the RuNPs displayed pertinent catalytic performances. Based on the TOF values, the relevant differences in terms of activity and selectivity highlighted the tuning of the catalytic performances of the nanocatalysts in the presence of cyclodextrin. The cyclodextrin acted as a phase-transfer promoter by increasing the activity of the reaction but also affected the selectivity. As evidenced by NMR studies, the influence on selectivity may result from the formation of an inclusion complex between the CD and the diphosphine ligand at the RuNPs surface, which modified their catalytic properties.

Taking advantage of the supramolecular properties of a cyclodextrin to modulate the surface reactivity of diphosphine-stabilized RuNPs, this original work may open up new opportunities in the field of nanocatalysis.

Experimental Section

Reagents and general procedures

All operations concerning nanoparticles syntheses were performed in Schlenck or Fischer–Porter glassware or in a glove box under argon atmosphere. The organometallic complex used as precursor, (1,5-cyclooctadiene)(1,3,5-cyclooctatriene)ruthenium(0) complex ([Ru(cod)(cot)]) was purchased from Nanomeps-Toulouse. Sulfonated diphosphine (1,4-bis[(di-*m*-sulfonatophenyl)phosphino]butane (L) was synthesized by following a published procedure^[7] and RAME- β -CD (Cavasol W7M) was purchased from Wacker Chemie GmbH in its pharmaceutical grade and was used as received. RAME- β -CD is a partially methylated β -cyclodextrin and its degree of substitution is equal to 1.8 per glucopyranose unit.^[15]

Solvents were dried and distilled before use: THF over sodium benzophenone and pentane over calcium hydride. All reagents and solvents were degassed before use by means of three freeze–pump–thaw cycles. Water was distilled twice by conventional method before use to prepare nanoparticle suspensions. Styrene and acetophenone used as substrates in catalysis were purchased from Acros Organics or Sigma-Alfa Aesar and used without further purification.

Characterization techniques

Samples for TEM/HRTEM analyses were prepared by slow evaporation of a drop of crude colloidal solution deposited onto holey carbon-covered copper grids under argon (in a glove box) for THF solutions and under air for aqueous solution. TEM and HRTEM analyses were performed at the Service Commun de Microscopie Electronique de l'Université Paul Sabatier (UPS–TEMSCAN). TEM images were obtained by using a JEOL 1011 electron microscope operating at 100 kV with resolution point of 4.5 Å. HRTEM observations were performed with a JEOL JEM 2010 electron microscope working at 200 kV with a resolution point of 2.5 Å. The diameter distributions were determined through manual analysis of enlarged micrographs with Imagetool software to obtain a statistical diameter distribution and a mean diameter (counting a minimum of 150 particles). FFT treatments were performed with Digital Micrograph Version 1.80.70.

¹H NMR, ¹³C {¹H} NMR, HSQC, COSY, and NOESY experiments were recorded on a Bruker Avance 500 spectrometer equipped with a 5 mm triple resonance inverse Z-gradient probe. All samples were prepared in D₂O. The 2D NOESY measurements were performed with a mixing time of 100 ms. All diffusion measurements were made by using the stimulated echo pulse sequence. The diffusion dimension was processed with single-exponential analysis involving least-squares fitting (Topspin software). Solid-state NMR experiments were recorded on a Bruker Avance 400 spectrometer equipped with a 4 mm probe. ³¹P CPMAS spectra were recorded with a recycle delay of 5 s and a contact time of 2 ms. ¹H and ³¹P chemical shifts are given relative to TMS and to an external 85% H₃PO₄ sample, respectively.

Elemental analyses (C, H, and N) were performed by the staff of Chemical Analyses Service of the LCC on a Eurovector 3011 instru-

ment. IR were run on a Perkin–Elmer FT spectrophotometer, series 2000 cm⁻¹ as KBr pellets or polyethylene films in the range 4000–150 cm⁻¹. Data collection for WAXS was performed at the CEMES CNRS (Toulouse) on small amounts of powder. All samples were sealed in 1 mm diameter Lindemann glass capillaries. The measurements of the X-ray intensity scattered by the samples irradiated with graphite monochromatized MoK α (0.071069 nm) radiation were performed by using a dedicated two-axis diffractometer. Measurement time was 15 h for each sample. Scattering data were corrected for polarization and absorption effects, then normalized to one Ru atom and Fourier transformed to obtain the radial distribution functions. To make comparisons with the crystalline structure in real space, a model was generated from bulk Ru parameters. The classic Debye's function was then used to compute intensity values subsequently Fourier transformed in the same conditions as the experimental ones.

Synthesis of ruthenium nanoparticles

The RuNPs system ([Ru]/[L]/[CD] = 1.0:0.1:1.0) has been chosen to describe the synthesis of the RuNPs, but all the syntheses performed were done in this way. In a typical reaction, Ru/0.1L/1.0CD, [Ru(cod)(cot)] (150 mg, 0.476 mmol) were introduced in a Fischer–Porter bottle and left in vacuum during 0.5 h and cooled to 193 K. THF (150 mL), containing a mixture of L (41 mg, 0.048 mmol, [L]/[Ru] = 0.1) and CD (640 mg, 0.048 mmol, [CD]/[Ru] = 1.0) were then added. The Fischer–Porter bottle was heated to 298 K and then pressurized with H₂ (3 bar). After 18 h, a homogenous brown colloidal solution was obtained. The volume of the solution was reduced to approximately 10 mL by solvent evaporation before its transfer onto a solution of deoxygenated pentane (100 mL). A brown precipitate formed, which was filtered and dried in vacuum, giving rise to the nanoparticles as a dark brown powder. The molar ratio of [L]/[Ru] was fixed to 0.1, taking account our previous results in catalysis,^[7] and the molar ratio of [CD]/[Ru] was varied from 0.2 to 5.0. In all cases, these ruthenium colloids were found to be stable with time under argon atmosphere without precipitation after several months. Inductively coupled plasma MS analysis for the different RuNPs: Ru/L (55.5 wt% Ru); Ru/L/0.2CD (22.1 wt% Ru); Ru/L/1.0CD (6.7 wt% Ru); Ru/L/5.0CD (1.5 wt% Ru).

Quantification of hydrides at the surface of ruthenium nanoparticles

The quantification of hydrogen atoms adsorbed onto the surface of Ru nanoparticles by gas chromatography (GC) analyses was performed on aqueous colloidal solutions by following a previously described procedure.^[7] On each fresh colloidal solution, 5.0 equivalents of olefin (2-norbornene), previously filtered through alumina, were added. Samples were taken from the solutions for GC analyses and estimation of the norbornene conversion into norbornane. The measurement of the amount of alkane formed by GC analysis allows determining the necessary quantity of hydrogen atoms for reducing the alkenes, and further to the H/surface Ru atomic ratio considering the nanoparticles mean diameters.

Gas chromatography was performed by using an HP 5890 Series II Gas Chromatograph with a SGE BP1 nonpolar 100% dimethyl polysiloxane capillary column of 50 m \times 0.32 mm \times 0.25 μ m. The method used for the quantification of hydrides consisted of 15 min at 40 °C and a ramp of 8 °C min⁻¹ until 250 °C. Conversions were determined as following: the peak area of the norbornane divided by the sum of the peak area of norbornene and norbornane.

Catalytic hydrogenation reactions

Gas chromatography

For all hydrogenation reactions, the conversion and the selectivity were determined by GC. A Carlo Erba GC 6000 with a flame ionization detector equipped with a Factor Four column (30 m, 0.25 mm inner diameter) was used for styrene hydrogenation analyses. Parameters were as follows: initial temperature, 40 °C; initial time, 10 min; ramp, 10 °C min⁻¹; final temperature, 80 °C; final time, 30 min; injector temperature, 220 °C; detector temperature, 250 °C. For acetophenone and *m*-methylanisole hydrogenation reactions, the reaction products were analyzed by using a Fisons Instrument GC 9000 series with a flame ionization detector equipped with a chiral Varian Chiralsil-Dex CB capillary column (30 m, 0.25 mm inner diameter). Parameters were as follows: isotherm program with oven temperature, 90 °C (*m*-methylanisole) or 130 °C (acetophenone); carrier gas pressure, 50 kPa.

Atmospheric hydrogenation reactions

A 25 mL round-bottom flask, charged with 10 mL of the colloidal suspension of Ru⁰NPs (10 mg) stabilized with the sulfonated diphosphine or with a mixture of sulfonated diphosphine–cyclodextrin and the appropriate amount of substrate (styrene, acetophenone, *m*-methylanisole) at RT was connected to a gas burette (500 mL) and a flask to balance pressure. Then, the system was filled with hydrogen ($P_{\text{H}_2} = 1$ bar) and the mixture was magnetically stirred at 1500 rpm. Samples were removed from time to time (2 h, 20 h, and 40 h) to monitor the reaction by GC in previously mentioned conditions.

High-pressure hydrogenation reactions

The stainless steel autoclave was charged with the aqueous suspension of the sulfonated diphosphine-stabilized or the sulfonated diphosphine–cyclodextrin-stabilized Ru⁰NPs and a magnetic stirrer at RT. The investigated substrate was added into the autoclave and was degassed three times. Finally, the hydrogen gas was admitted to the system at a constant pressure (10 bar H₂). The mixture was stirred vigorously at RT. Samples were removed from time to time (2 h, 20 h, and 40 h) to monitor the reaction by GC in previously mentioned conditions.

Acknowledgements

The authors thank V. Collière and L. Datas (LCC–CNRS and UPS–TEMSCAN) for TEM/HRTEM facilities. The authors are grateful to CNRS and the Agence Nationale de la Recherche (ANR-09-BLAN-0194) for the financial support of the SUPRANANO program.

Keywords: cyclodextrins • nanoparticles • phosphanes • ruthenium • supramolecular chemistry

[1] *Nanoparticles: From Theory to Application*, 2nd ed. (Ed.: G. Schmid), Wiley-VCH, Weinheim, 2012.

- [2] a) *Nanoparticles and Catalysis* (Ed.: D. Astruc), Wiley-VCH, Weinheim, 2008; b) Z. X. Li, W. Xue, B. T. Guan, F. B. Shi, Z. J. Shi, H. Jiang, C. H. Yan, *Nanoscale* 2013, 5, 1213–1220.
- [3] *Nanomaterials in Catalysis* (Eds.: P. Serp, K. Philippot), Wiley-VCH, Weinheim, 2013.
- [4] P. Lara, K. Philippot, B. Chaudret, *ChemCatChem* 2013, 5, 28–45.
- [5] a) C. Burda, X. Chen, R. Narayanan, M. A. El-Sayed, *Chem. Rev.* 2005, 105, 1025–1102; b) A. Gual, C. Godard, K. Philippot, B. Chaudret, A. Denicourt-Nowicki, A. Roucoux, S. Castillón, C. Claver, *ChemSusChem* 2009, 2, 769–779; c) M. Zahmakiran, M. Tristany, K. Philippot, K. Fajerweg, S. Özkar, B. Chaudret, *Chem. Commun.* 2010, 46, 2938–2940; d) E. Guyonnet Bilé, E. Cortelazzo-Polisini, A. Denicourt-Nowicki, R. Sassine, F. Launay, A. Roucoux, *ChemSusChem* 2012, 5, 91–101; e) E. Guyonnet Bilé, A. Denicourt-Nowicki, R. Sassine, F. Launay, A. Roucoux, *Dalton Trans.* 2011, 40, 6524–6531; f) D. Gonzalez-Galvez, P. Lara, O. Rivada-Wheekaghan, S. Conejero, B. Chaudret, K. Philippot, P. N. M. W. Van Leeuwen, *Catal. Sci. Technol.* 2013, 3, 99–105; g) D. Peral, F. Gómez-Villarraga, J. García-Antón, X. Sala, J. Pons, J. Carles Bayón, J. Ros, M. Guerrero, L. Vendier, P. Lecante, K. Philippot, *Catal. Sci. Technol.* 2013, 3, 475–489.
- [6] P.-J. Debouttière, V. Martinez, K. Philippot, B. Chaudret, *Dalton Trans.* 2009, 10172–10174.
- [7] M. Guerrero, A. Roucoux, A. Denicourt-Nowicki, H. Bricout, E. Monflier, V. Collière, K. Fajerweg, K. Philippot, *Catal. Today* 2012, 183, 34–41.
- [8] a) F. Hapiot, A. Ponchel, S. Tilloy, E. Monflier, *C. R. Chim.* 2011, 14, 149–166; b) H. Bricout, F. Hapiot, A. Ponchel, S. Tilloy, E. Monflier, *Curr. Org. Chem.* 2010, 14, 1296–1307; c) F. Hapiot, L. Leclercq, N. Azaroual, S. Fourmentin, S. Tilloy, E. Monflier, *Curr. Org. Synth.* 2008, 5, 162–172.
- [9] a) A. Nowicki, Y. Zhang, B. Léger, J. P. Rolland, H. Bricout, E. Monflier, A. Roucoux, *Chem. Commun.* 2006, 296–298; b) A. Denicourt-Nowicki, A. Ponchel, E. Monflier, A. Roucoux, *Dalton Trans.* 2007, 5714–5719; c) C. Hubert, A. Denicourt-Nowicki, A. Roucoux, D. Landy, B. Leger, G. Crowyn, E. Monflier, *Chem. Commun.* 2009, 1228–1230; d) R. Herbois, S. Noël, B. Léger, L. Bai, A. Roucoux, E. Monflier, A. Ponchel, *Chem. Commun.* 2012, 48, 3451–3453; e) N. T. T. Chau, S. Handjani, J.-P. Guegan, M. Guerrero, E. Monflier, K. Philippot, A. Denicourt-Nowicki, A. Roucoux, *ChemCatChem* 2013, 5, 1497–1503.
- [10] a) M. Ferreira, H. Bricout, A. Sayede, A. Ponchel, S. Fourmentin, S. Tilloy, E. Monflier, *Adv. Synth. Catal.* 2008, 350, 609–618; b) L. Caron, H. Bricout, S. Tilloy, D. Landy, S. Fourmentin, E. Monflier, *Adv. Synth. Catal.* 2004, 346, 1449–1456; c) C. Binkowski, J. Cabou, H. Bricout, F. Hapiot, E. Monflier, *J. Mol. Catal. A-Chem.* 2004, 215, 23–32; d) M. Canipelle, L. Caron, C. Christine, S. Tilloy, E. Monflier, *Carbohydr. Res.* 2002, 337, 281–287.
- [11] a) J. García-Antón, M. Rosa Axet, S. Jansat, K. Philippot, B. Chaudret, T. Pery, G. Buntkowsky, H.-H. Limbach, *Angew. Chem.* 2008, 120, 2104–2108; *Angew. Chem. Int. Ed.* 2008, 47, 2074–2078; b) D. González-Gálvez, P. Nolis, K. Philippot, B. Chaudret, P. W. N. M. van Leeuwen, *ACS Catal.* 2012, 2, 317–321.
- [12] a) E. Ramírez, L. Eradès, K. Philippot, P. Lecante, B. Chaudret, *Adv. Funct. Mater.* 2007, 17, 2219–2228; b) E. Ramírez, S. Jansat, K. Philippot, P. Lecante, M. Gómez, A. M. Masdeu-Bultó, B. Chaudret, *J. Organomet. Chem.* 2004, 689, 4601–4610.
- [13] B. Fritzing, I. Moreels, P. Lommens, R. Koole, Z. Hens, J. C. Martins, *J. Am. Chem. Soc.* 2009, 131, 3024–3032.
- [14] A. Kalantar Neyestanaki, P. Maki-Arvela, H. Backman, H. Karhu, T. Salmi, J. Vayrynen, D. Y. Murzin, *J. Catal.* 2003, 218, 267–279.
- [15] a) M. Ferreira, F. X. Legrand, C. Machut, H. Bricout, S. Tilloy, E. Monflier, *Dalton Trans.* 2012, 41, 8643–8647; b) F. X. Legrand, M. Sauthier, C. Fla-haut, J. Hachani, C. Elfakir, S. Fourmentin, S. Tilloy, E. Monflier, *J. Mol. Catal. A-Chem.* 2009, 303, 72–77.

Received: June 17, 2013

Published online on September 20, 2013